Journal of Molecular Graphics and Modelling 59 (2015) 31–39

Contents lists available at ScienceDirect

Journal of Molecular Graphics and Modelling

journal homepage: www.elsevier.com/locate/JMGM

Theoretical design and simulation of supramolecular polymer unit based on multiple hydrogen bonds

Haijie Shi[a,b], Fengdi Wang[a,b], Wei Chen[a,b], Shuwei Tang[a,b], Wanqiao Zhang[a,b], Wenliang Li[a], Hao Sun[a,b,*], Jingping Zhang[a,*], Rongshun Wang[a,b,*]

[a] Institute of Functional Material Chemistry, Faculty of Chemistry, Northeast Normal University, Renmin Road 5268, Changchun, Jilin 130024, P.R. China
[b] National & Local United Engineering Lab for Power Battery, Northeast Normal University, Renmin Road 5268, Changchun, Jilin 130024, P.R. China

ARTICLE INFO

Article history:
Received 1 February 2015
Received in revised form 24 March 2015
Accepted 26 March 2015
Available online 3 April 2015

Keywords:
Hydrogen bonds
Heterocycles
DFT
Stability

ABSTRACT

The heterocyclic urea of deazapterin (**DeAP *a***) and its protomeric conformers (***b***, ***c***) with different substituents are selected as the building block for a series of dimers in different configurations. The stabilities of all dimers in various conditions have been investigated by density functional theory. Homodimer of ***b*** has more stability than other dimers. Topological analyses certify the coexistence of intermolecular with intramolecular H-bonds. Investigations into frequency demonstrate that all H-bonds show an evident red shift in their stretching vibrational frequencies. Electron donating substituents can provide favorable free energies of the dimer. Solvent effect computations suggest that the dimerization can be favored in weakly polar solvents, such as toluene and chloroform. UV–visible spectra exhibit obvious difference of maximum absorption wavelengths between monomers and dimers, thus may have potential applications for identifying intermolecular H-bonds and calculating association constant of **DeAP** equilibrium systems in experiments.

1. Introduction

Recently, considerable progress has been achieved on design of novel supramolecular materials based on multi-point hydrogen-bonding motifs [1–11]. Owing to its directionality and strength, the hydrogen bond has become an ideal candidate for the noncovalent assembly of supramolecular and biological macromolecular (e.g., nucleic acids and proteins) building blocks [12–15]. Recent years, many researchers dedicated to designing and synthesizing molecules based on hydrogen-bonded modules with donor (D) and acceptor (A) functionalities [16]. By introducing more donor and acceptor sites into arrays, the strength of hydrogen bonds in polymers can be improved and then the selectivity are enhanced between two arrays. Once the hydrogen-bonded motifs interact, they can aggregate via two patterns: homodimers, when two equal units integrate in the way that the arrangement of the interacting functionalities (D or A) is self-complementary; heterodimers, when two different units integrate in a complementary way of their functionalities.

Among the reversible and directional multiple hydrogen bonds, quadruple hydrogen-bonding arrays have been successfully applied in generating supramolecular polymers. In the past several decades, the self-complementary ureidopyrimidone [17–19] and ureidodeazapterin [20–24] units are the most successful in extensive research areas (notably in producing supramolecular polymers) for their strong affinity and synthetic accessibility. Heterocyclic urea of **DeAP *a*** (and its protomeric conformer ***b***) (Fig. 1) containing self-complementary AADD hydrogen-bonding sites, was developed by Zimmerman's group [20a] without consideration of sits protomeric form. It can generate exceedingly strong quadruple hydrogen-bonding hetero- and homodimers ($K_{dim} > 10^7\ M^{-1}$ in chloroform, among the largest association constant reported to date for neutral, hydrogen-bonding materials) with similar spatial arrangement of alkyl substituents, which is significant for applications in self-assembly. **DeAP *a***, soluble in nonpolar organic solvents, can be obtained conveniently by heating 2-amino-3H-pyrido-(2,3-*d*)pyrimidin-4-one, which is available in a two-step synthesis from commercially available 2,4-diamino-6-hydroxypyrimidine [25], and butylisocyanate. As shown in Fig. 1, **DeAP *a*** has four different tautomers in solution, which can dimerize to homo- or heterodimeric AADD–DDAA or DADA–ADAD arrays

* Corresponding authors at: Institute of Functional Material Chemistry, Faculty of Chemistry, Northeast Normal University, Renmin Road 5268, Changchun, Jilin 130024, P.R. China. Tel.: +86 043185099291.
E-mail addresses: sunh600@nenu.edu.cn (H. Sun), zhangjp@nenu.edu.cn (J. Zhang), wangrs@nenu.edu.cn (R. Wang).

http://dx.doi.org/10.1016/j.jmgm.2015.03.004
1093-3263/

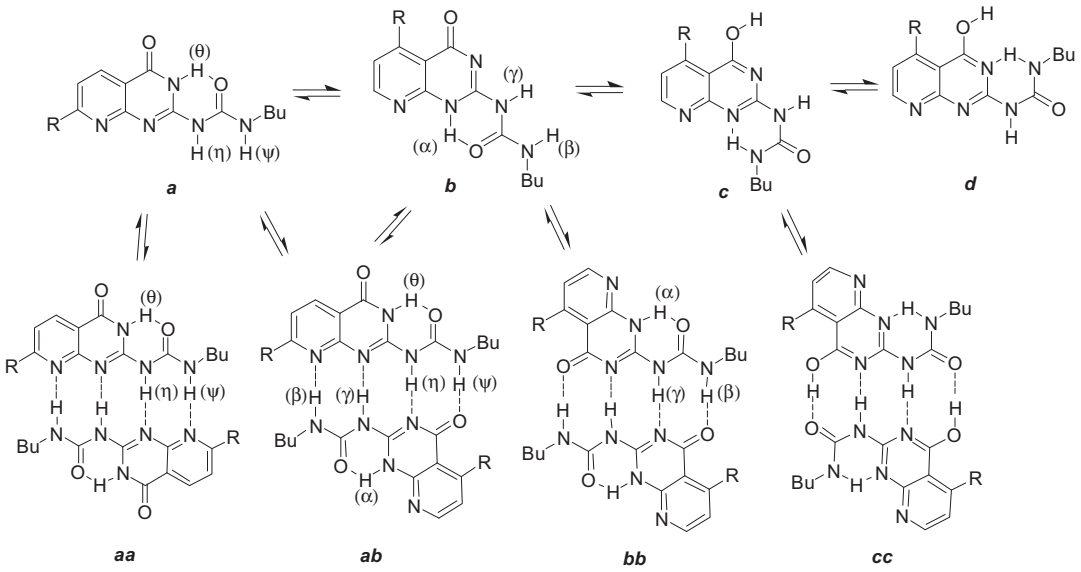

Fig. 1. Conformational, protomeric, and self-association equilibria of module ***a***.

via quadruple hydrogen-bondings, except for ***d***, a minor form which cannot form quadruple hydrogen bonded dimeric structure.

The synthetic accessibility of **DeAP *a*** and ***b***, and the exceedingly strong H-bonds in corresponding complexes, make them promising modules for the construction of supramolecular oligomers and polymers. Although there is remarkable progress in the experimental aspect, few systematic theoretical studies have been reported [26], especially about the effect of solvent and substitution groups adjacent to the hydrogen bonds on the stability of dimers. Since electron donating substituents generally favor binding energies and free energies of dimerization, we introduced four hydrophobic and electron donating groups (R = methyl, propyl, *n*-butyl and iso-butyl) into the adjacent position of the quadruple hydrogen bonds, in the aim to protect the quadruple hydrogen bonds from damaging by the solvent molecules and further achieve more stable dimers.

In order to better understand the nature of hydrogen bonds theoretically, we will discuss the interactions of a series of dimers in different configurations (***aa***, ***ab***, ***bb***, ***cc***) based on **DeAP *a*** and its protomeric conformers, involving interaction energies, interactions between accepting and donating orbitals of H-bonds and electronic properties of dimers. In addition, we will also report the effect of substitution groups adjacent to the hydrogen bonds and solvents on the stability of dimers.

2. Computational details

The density functional theory (DFT) has emerged during the past decades as a powerful methodology for the simulation of chemical systems. Despite taking less comprehensive electron correlations into consideration than the Second-order Moller-Plesset perturbation theory (MP2) method, DFT methods have been proved to characterize weak interactions sufficiently [26c,e,d,–28]. PBE1PBE [29–33], the hybridized function of GGA type, performed very well when dealing with hydrogen bonds energy in complexes. To test the applicability of the PBE1PBE functional in this research, we also considered alternative functional for the optimization calculations. Five functionals including PBE1PBE, X3LYP [34], M06-2X [35], ωB97XD [36] and B3LYP [37] were used to optimize the structure of DDAA–AADD hydrogen-bonded **UPy** dimer, which was widely used and available for experimental geometric parameters from Meijer's group [17b], with the same 6-31+G(d,p) basis set (Table S1 (Supporting Information) and Scheme S1). It showed that geometric parameters from PBE1PBE and **ω**B97XD fitted much better with experimental data than other functional. Although **ω**B97XD actually gives more accurate results than PBE1PBE, the latter may perform faster and can be compared to previous studies more easily. Therefore, the PBE1PBE method was used to perform the geometry optimizations. All the calculations have been done with Gaussian09 [38] program, unless specified otherwise. To find proper basis set for systems investigated here, we conducted comparison analysis between the PBE1PBE/6-31G(d) geometry of the unsubstituted dimers (R = H) and those derived from higher level PBE1PBE/6-31+G(d,p) for available structures. It showed that PBE1PBE/6-31G(d) optimization can provide credible results with the insignificant geometry differences between the two computational levels which were less than 1.38% (Fig. S1). Geometry optimizations of monomers and dimers were carried out at the PBE1PBE/6-31G(d) level taking into account the balance between the computational economy and the accuracy. Frequency calculations were performed on all optimized geometries at the same level to verify the nature of all stationary points as minima. Based on the optimized configuration, we used the PBE1PBE/6-311++G(2df,2p) level for the single point energy calculations and the NPA analysis. The predictions of NMR and UV/visible absorption spectrum were calculated at the same level.

The effect of solvent was considered for geometric optimization and single point energy calculations, using polarizable continuum models (PCM) [39,40]. In the calculation of weak interactions such as multiple hydrogen bonding systems studied here, basis set superposition error (BSSE) would take up a considerable proportion and even lead to errors. Therefore, BSSE correction was calculated herein for all computations by the counterpoise (CP) method [41,42] of Boys and Bernardi based on the optimized structures. Since the CP method is incompatible with the PCM model, BSSE calculations for dimers in various solvents were conducted without applying the PCM model. To estimate the strength of hydrogen bonds, we calculated the binding energy with BSSE and zero-point energy (ZPE) corrections. To get a further understanding of hydrogen bonds in this work, the topological properties of electron densities for the monomers and complexes were computed at the PBE1PBE/6-311++G(2df,2p) level by combining Gaussian09 with Multiwfn3.3 [43–45] program.

3. Results and discussion

3.1. Geometric configuration of monomers and dimers

The structural parameters and vibrational frequencies of H-bonds in all the monomers and dimers are summarized in Table S2 and Table 1, respectively. From Zimmerman's work [20a], the minor protomer ***c***, containing self-complementary DADA hydrogen-bonding array, formed dimer ***cc*** with the relative percentage 2% in toluene-d_8 and 6% in $CDCl_3$. Consequently, the focal point in our following discussion will be mainly concentrate on other relatively major monomers and dimers containing DDAA–AADD arrays, namely, in ***aa***, ***ab***, and ***bb*** form.

As shown in Table S2 and Fig. S2, all three N—H bonds are lengthened when the monomers create corresponding dimers in various surroundings (vacuum, toluene, chloroform, and water). The greatest change of all N—H bond lengths is found in a vacuum. The increase of N—H(α/θ) bond lengths is larger in toluene than in chloroform and water. However, no evident change is found for N—H(β/Ψ) and N—H(γ/η) bonds in various solvents. The N—H(β/Ψ) and N—H(γ/η) bonds are lengthened more than the N—H(α/θ) bond in each condition. The lengths between H(α/θ) and O(α/θ) get shorter when dimers generated, whereas the decrement turns smaller when the polarity of solvents increase, that is, in the order of vacuum > toluene > chloroform > water. Table S2 and Fig. S2 indicate that the distances between H(α) and O(α) in dimers in ***bb*** form range from 1.737 to 1.748 Å in a vacuum, from 1.743 to 1.753 Å in toluene, from 1.746 to 1.756 Å in chloroform and from 1.750 to 1.759 Å in water, which are classical hydrogen bond lengths [46] and less than the sum of van der Waals radii [47] (for H. . .O, 2.5 Å; for H. . .N, 2.6 Å). More detailed certification of hydrogen bonds will be discussed below. All N—H(α). . .O bond lengths in dimers in ***bb*** form are almost same with the corresponding N—H(β). . .O bonds, but in ***ab*** form, the latter is larger than the former. The largest bond length of all three hydrogen bonds in different surroundings observed is N—H(γ/η). . .N bonds. For instance, N—H(α). . .O and N—H(γ). . .N hydrogen bonds of dimers in ***bb*** form (R = butyl) are 1.747 and 1.997 Å in a vacuum, 1.752 and 2.004 Å in toluene, 1.755 and 2.007 Å in chloroform, and 1.758 and 2.009 Å in water, respectively. The resulting values reveal that solvent influence the hydrogen bonds remarkably. Since dimers in ***aa*** form are less major than dimers in the other two forms (see below for details in the energy part), we mainly discuss the effect of substituents on dimers in ***bb*** and ***ab*** form. Considering the influence of the substituents herein, larger substituents possess stronger electron donating ability and in principle result in shorter H-bonds. Interestingly, the hydrogen bonds are quite similar instead of shortening with the increasing size of substituent groups.

From Table 1, we can see that all dimers exhibit substantially decreased stretching frequencies for the N—H bonds in hydrogen bonds compared with monomers, suggesting an obvious red shift of their IR spectrum. The largest change can be found in N—H(β), then N—H(γ) and lastly N—H(α) in dimers in ***bb*** form. Most importantly, the red shifts of N—H(β) and N—H(γ) increase with the increasing size of substituent groups, except for N—H(γ) in a vacuum. Nevertheless, there is a reversal in N—H(α). This is probably because that the charge rearrangement caused by substitution groups has affected intermolecular and intramolecular hydrogen bonds in different ways (the former is strengthened and the latter is weakened). More details of the vibrational stretching frequencies for the N—H bonds in dimers in ***aa*** and ***ab*** form can be seen in Table S3. For comparison, we also added the vibrational frequency calculation of the dimer-**UPy** (Scheme S1) whose experimental vibrational frequency data are available [48] at the PBE1PBE/6-31G(d) level. Calculated hydrogen-bonding NH group stretching correspond to 3259 and 3205 cm^{-1} in chloroform, which are in good agreement

Table 1
Vibrational stretching frequencies (cm^{-1}) for N—H(α), N—H(β), and N—H(γ) Bonds in ***b*** and ***bb***[a] forms (values in parentheses are the corresponding IR intensities (km/mol)).

		Vacuum			Toluene			Chloroform			Water		
R		N—H(α)	N—H(β)	N—H(γ)	N—H(α)	N—H(β)	N—H(γ)	N—H(α)	N—H(β)	N—H(γ)	N—H(α)	N—H(β)	N—H(γ)
H	***b***	3479 (403)	3660 (55)	3642 (34)	3459 (520)	3660 (91)	3641 (41)	3445 (590)	3659 (112)	3640 (49)	3434 (675)	3661 (126)	3637 (76)
	bb	3306 (1260)	3327 (5185)	3327 (5185)	3318 (2360)	3316 (5080)	3316 (5080)	3325 (1675)	3310 (6273)	3310 (6273)	3333 (1818)	3302 (6764)	3302 (6764)
		[−173]	[−333]	[−333]	[−141]	[−344]	[−325]	[−120]	[−349]	[−330]	[−101]	[−359]	[−335]
Me	***b***	3488 (399)	3660 (54)	3643 (33)	3468 (513)	3662 (77)	3644 (53)	3458 (579)	3663 (93)	3642 (67)	3444 (668)	3661 (116)	3639 (85)
	bb	3321 (1276)	3327 (5236)	3327 (5236)	3334 (1502)	3315 (6048)	3315 (6048)	3341 (1615)	3308 (6426)	3308 (6426)	3350 (1769)	3300 (6869)	3300 (6869)
		[−167]	[−333]	[−316]	[−134]	[−347]	[−329]	[−117]	[−355]	[−334]	[−94]	[−361]	[−339]
Pr	***b***	3489 (414)	3661 (53)	3643 (33)	3469 (527)	3665 (63)	3645 (70)	3458 (592)	3666 (76)	3644 (85)	3446 (678)	3664 (106)	3640 (97)
	bb	3325 (1795)	3327 (4768)	3327 (4768)	3336 (1534)	3315 (6162)	3315 (6162)	3343 (1651)	3308 (6642)	3308 (6642)	3351 (1801)	3300 (7230)	3300 (7230)
		[−164]	[−334]	[−316]	[−133]	[−350]	[−330]	[−115]	[−358]	[−336]	[−95]	[−364]	[−340]
Bu	***b***	3489 (420)	3661 (53)	3643 (34)	3469 (532)	3665 (60)	3646 (71)	3459 (593)	3666 (75)	3644 (86)	3446 (679)	3664 (107)	3641 (97)
	bb	3325 (1982)	3327 (4612)	3327 (4612)	3336 (1548)	3315 (6145)	3315 (6145)	3342 (1664)	3309 (6626)	3309 (6626)	3350 (1812)	3300 (7224)	3300 (7224)
		[−164]	[−334]	[−316]	[−133]	[−350]	[−331]	[−117]	[−357]	[−335]	[−96]	[−364]	[−341]
iBu	***b***	3489 (420)	3661 (54)	3643 (33)	3470 (532)	3665 (59)	3646 (70)	3459 (595)	3666 (73)	3645 (85)	3446 (680)	3663 (108)	3641 (93)
	bb	3323 (1522)	3328 (5078)	3328 (5078)	3334 (1565)	3316 (6117)	3316 (6117)	3341 (1678)	3310 (6577)	3310 (6577)	3348 (1830)	3302 (7162)	3302 (7162)
		[−166]	[−333]	[−315]	[−136]	[−349]	[−330]	[−118]	[−356]	[−335]	[−98]	[−361]	[−339]

[a] The decrease of the stretching frequencies is listed in square brackets.

with experimental results (3212 and 3147 cm^{-1}), proving that the economic PBE1PBE functional combining with 6-31G(d) basis sets performed well on predicting the vibrational frequency of such hydrogen-bonded dimers.

3.2. Energies

3.2.1. Energy of monomers and dimers

In order to rationalize and interpret the experimental results, single point energies of hydrogen-bonding complexes between ***a*** and its conformers were computed at the PBE1PBE/6-311++G(2df,2p) level on the basis of optimized structures at the PBE1PBE/6-31G(d) level. The calculated BSSE, ZPE and energies of all monomers and dimers along with the binding energies and free energies for dimerization of ***aa***, ***ab***, and ***bb*** forms are gathered in Table 2 and Table S4. As a result, for unsubstituted monomer, ***a*** has slightly lower energy than ***b***, and for dimer, the stability in various environments (except in water) is as follows: ***bb*** > ***ab*** > ***aa***. Since dimers in ***aa*** form are less major than other two forms, we mainly discuss the effect of substituents on ***ab*** and ***bb***. Moreover, for substituted ones (R = methyl, propyl, *n*-butyl, iso-butyl), monomer ***a*** still remains the most favorable form, but the relative stability of dimers become ***ab*** > ***bb***, though the difference of energy values is quite small. It is shown that the stability of the dimers depends not only on solvent, but also on substituent. For instance, the energies of dimers in ***bb*** form (R = H) are 1.51, 0.82, and 0.38 kcal/mol lower than those of the corresponding dimers in ***ab*** form (R = H) in a vacuum, toluene and chloroform, respectively, but is 0.19 kcal/mol higher in water. The energies of dimers in ***ab*** form (R = Me) are 0.19, 1.13, 1.69, and 6.28 kcal/mol lower than those of the corresponding dimers in ***bb*** form (R = Me) in a vacuum, toluene, chloroform and water, respectively. As a matter of fact, the methyl group can stabilize dimers in ***ab*** form (R = Me) better than ***bb*** form (R = Me) especially in polar solvent. In view of the energy, **DeAP** ***a*** and its conformers prefer to form homodimers in ***bb*** form without substituents, whereas, substituents are not favorable for the stability of ***bb***.

3.2.2. Interaction energy of dimers

As shown in Table S4, there is no significant change for BSSE values with increasing size of substituents and solvents, ranging from 1.09 to 1.30 kcal/mol for dimers in ***ab*** form, from 1.09 to 1.19 kcal/mol for dimers in ***bb*** form at the PBE1PBE/6-311++G(2df,2p) level. Moreover, it is interesting to note that larger electron donating substitution groups do not necessarily mean larger binding energies. For example, the binding energies in a vacuum are −36.80, −36.06, −36.11, −36.08, and −36.11 kcal/mol for dimers in ***bb*** form (R = H, Me, Pr, Bu, *i*Bu), respectively. Two possible reasons [49] cause such trend: in one respect, the steric crowding derived from substituents (Me, Pr, Bu, *i*Bu) may hinder the dimerization process; on the other hand, the weak C—H. . .O interaction between substituents (Me, Pr, Bu, *i*Bu) and O(β) may weaken intermolecular hydrogen bonds, further reduce the stability of dimers. Actually, the nature of solvent is vital for the binding energy of dimerization. For dimers in ***ab*** form (R = Bu), the binding energies are −31.98 kcal/mol in a vacuum, −24.96 kcal/mol in toluene, −21.13 kcal/mol in chloroform and −16.28 kcal/mol in water, respectively, which are comparable with the famous **UPy**-based strong hydrogen-bonding dimers (Table S5) and in good agreement with the experiment that possessing extremely large dimerization constant ($K_{dim} > 10^7\ M^{-1}$) [20a]. Consequently, high polar solvents interfere with the formation of stable dimers, which can be confirmed in later discussion (solvent effects section).

According to Table 2 and Fig. 2, the binding energy of dimers in ***bb*** form is always larger than dimers in ***ab*** form

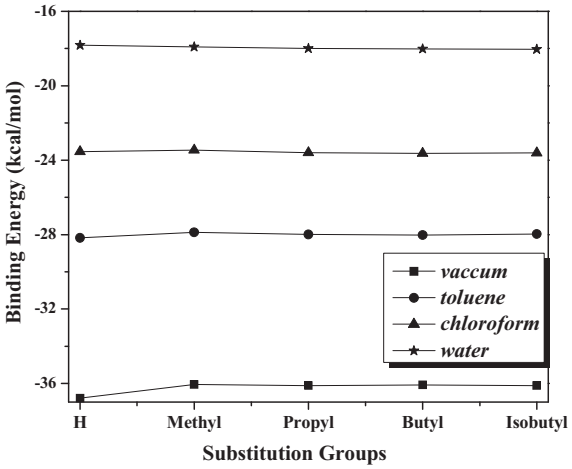

Fig. 2. Binding energies of dimer ***bb*** with different substituents in various environments.

in various conditions. Considering the possible effect of solvation models, we also calculated the binding energies for dimerization processes using the SMD and CPCM models at PBE1PBE/6-311++G(2df,2p)//PBE1PBE/6-31G(d) level in toluene and chloroform. The detailed results are gathered in Fig. S3, indicating that hydrogen bonds in dimers in ***bb*** form are all stronger than ***ab*** form from different methods and solvation models, which is consistent with the experiment that the K_{dim} for ***bb*** is slightly larger [20a].

Furthermore, Table 2 lists the free energies of dimerization of hydrogen bonding complexes in various environments with BSSE and ZPE corrections. From Table 2 and Fig. 3, it shows that the free energies of dimerization are negative in various surroundings, but a small positive value (0.27 kcal/mol) of dimer in ***ab*** form (R = *iso*butyl) in water is an exception. The free energies of all dimerization processes decrease with the increasing polarity of solvent, namely, vacuum > toluene > chloroform > water, implying different practicability and accessibility of dimerization in different solvents. Additionally, larger substituents correspond to slightly larger negative free energies, indicating that dimerization may be motivated by hydrophobic groups near the hydrogen bonds. Since the dimers in ***bb*** form are stable than the ***ab*** form in various conditions, the following parts will focus mainly on ***bb***.

Moreover, as shown in Table 2, we also calculated binding energies ($\mathbf{E_{b\text{-}PCM}}$) and free energies ($\mathbf{\Delta G_{PCM}}$) without BSSE

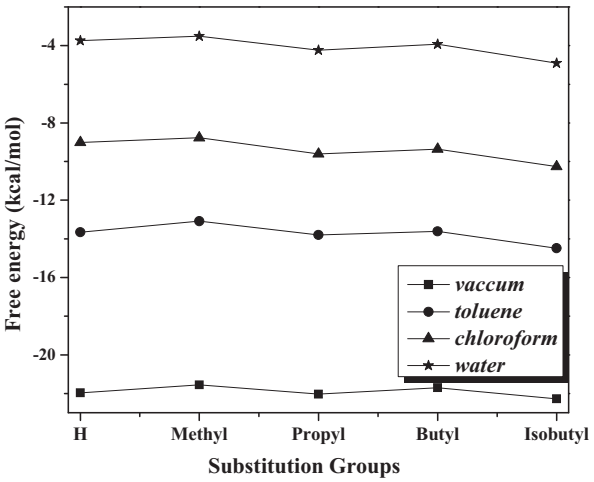

Fig. 3. Free energies of dimer ***bb*** in various environments.

Table 2
Binding energies and free energies (298 K) for dimerization at the PBE1PBE/6-311++G(2df,2p) level (unit: kcal/mol)[a].

		Vacuum		Toluene				Chloroform				Water			
R		E_b	ΔG	E_b	$E_{b\text{-}PCM}$	ΔG	ΔG_{PCM}	E_b	$E_{b\text{-}PCM}$	ΔG	ΔG_{PCM}	E_b	$E_{b\text{-}PCM}$	ΔG	ΔG_{PCM}
H	***aa***	−29.77	−15.43	−23.54	−24.63	−9.06	−10.15	−20.15	−21.25	−5.68	−6.78	−16.01	−17.10	−1.86	−2.96
	ab	−33.21	−19.27	−25.82	−26.92	−11.74	−12.84	−21.84	−22.93	−7.62	−8.72	−16.92	−18.01	−3.23	−4.32
	bb	−36.80	−21.96	−28.18	−29.28	−13.66	−14.76	−23.54	−24.64	−9.01	−10.11	−17.82	−18.92	−3.74	−4.84
Me	***ab***	−31.35	−16.14	−24.23	−25.42	−8.05	−9.25	−20.45	−21.64	−4.63	−5.83	−15.83	−17.03	−0.39	−1.58
	bb	−36.06	−21.56	−27.87	−29.06	−13.08	−14.27	−23.46	−24.64	−8.77	−9.95	−17.92	−19.10	−3.52	−4.70
Pr	***ab***	−31.91	−16.26	−24.84	−26.11	−9.23	−10.51	−20.98	−22.26	−5.45	−6.73	−16.12	−17.40	−0.52	−1.80
	bb	−36.11	−22.04	−28.00	−29.18	−13.80	−14.98	−23.60	−24.78	−9.61	−10.79	−18.00	−19.18	−4.24	−5.42
Bu	***ab***	−31.98	−16.86	−24.96	−26.25	−9.82	−11.12	−21.13	−22.43	−6.00	−7.30	−16.28	−17.57	−0.93	−2.23
	bb	−36.08	−21.70	−28.02	−29.20	−13.62	−14.80	−23.64	−24.82	−9.36	−10.54	−18.02	−19.20	−3.92	−5.10
iBu	***ab***	−29.78	−14.74	−23.07	−24.34	−8.11	−9.37	−19.39	−20.65	−4.53	−5.79	−14.57	−15.83	0.27	−0.99
	bb	−36.11	−22.28	−27.97	−29.15	−14.49	−15.67	−23.61	−24.79	−10.26	−11.44	−18.04	−19.22	−4.91	−6.09

[a] $E_{b\text{-}PCM}$ and ΔG_{PCM} are the results with the PCM model and ZPE corrections, others are results with BSSE and ZPE corrections.

corrections for comparison. As expected, energy values are overestimated resulting from neglecting BSSE corrections (the actual binding energies and free energies are not so large negative values).

3.2.3. Solvent effects

To elucidate the solvent effect on dimerization, we next introduced the accurate "implicit-explicit" model [50–52], surrounding the explicit solvent molecule with a continuum solvent model, into the analysis of competitive interactions between monomer in ***b*** form (R = H) and solvent molecules (water and chloroform). In this model, solutes combined with different numbers of explicit solvent molecules are taken as a complex in continuum solvent. We can derive the initial complexes from adding different numbers (n = 1–4) of water or chloroform molecules around the monomer in ***b*** form manually. Calculations on the complexes were performed at the PBE1PBE/6-311++G(2df,2p)//PBE1PBE/6-31G(d) level with PCM model. As mentioned above, the energies here were also corrected with BSSE and ZPE correction. Quantitative representative analysis of the interactions will be discussed in Fig. 4 in the light of

$$E_b = E(\text{complex}) - E(\text{monomer}(b)) - E(\text{solvents}) \quad (1)$$

It should be highlighted that E (solvents) is the total energy of solvent molecules around ***b*** on the basis of the structure in the corresponding complex. The most stable configurations and binding energies of complexes in Fig. 4 demonstrate the adverse effect of water molecules upon the dimerization of **DeAP** ***b***. For n = 1, the docking site possessing two NH...O (E_b = −3.71 kcal/mol) H-bonds is much stable than the one with OH...O and OH...N (E_b = −2.88 kcal/mol) H-bonds. As expected, more solvent molecules correspond to larger binding energies for the complex. For example, the binding energies between **DeAP** ***b*** and water molecules are −3.71, −8.36, −10.95 and −15.29 kcal/mol for n = 1, 2, 3, and 4, respectively. The comparative values of E_b [$(H_2O)_4$] and binding energy of dimers in ***bb*** form (−17.82 kcal/mol) in water suggest that water molecules compete by hydrogen bonding with dimers of ***b***, this may leads to lowered dimerization constants or hydrolysis of the dimer. Nevertheless, the binding energies for complexes based on ***b*** and $CHCl_3$ molecules are E_b [$(CHCl_3)_1$] = −3.38 kcal/mol and E_b [$(CHCl_3)_2$] = −4.31 kcal/mol, respectively, showing that the dimerization (E_b = −23.54 kcal/mol) is dominant over the interactions between ***b*** and solvent molecules. Therefore, **DeAP** ***b*** tends to form stable dimers in relatively less polar solvents (such as chloroform), which agrees well with the experiment that hydrogen-bonded complexes have been usually explored in chloroform [20a].

3.3. Natural bond orbital analysis

Natural bond orbital analysis provides an efficient method for investigating charge delocalization and conjugative interactions in hydrogen-bonding complexes. The second-order perturbation approach [53] was applied to estimate the acceptor-donor interactions in hydrogen-bonding arrays quantitatively. For each donor (i) and acceptor (j) natural bond orbital, the stabilization energy (hyperconjugative interaction energy) between donor and acceptor was evaluated as

$$E(2) = \Delta E_{ij} = m_i \frac{F(i,j)^2}{\varepsilon_j - \varepsilon_i} \quad (2)$$

where m_i is the occupancy of the donor orbital, ε_i and ε_j are diagonal elements (orbital energies), and $F(i, j)$ is the off diagonal Fock matrix element between i and j NBO orbitals, respectively. In

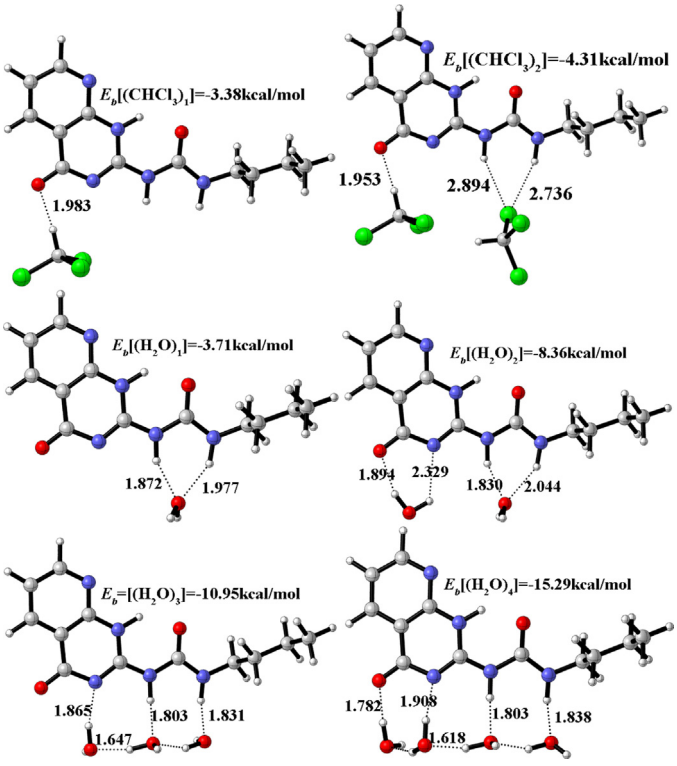

Fig. 4. Geometries and binding energies of complexes of urea ***b*** interacting with different numbers of solvent molecules (unit: Å).

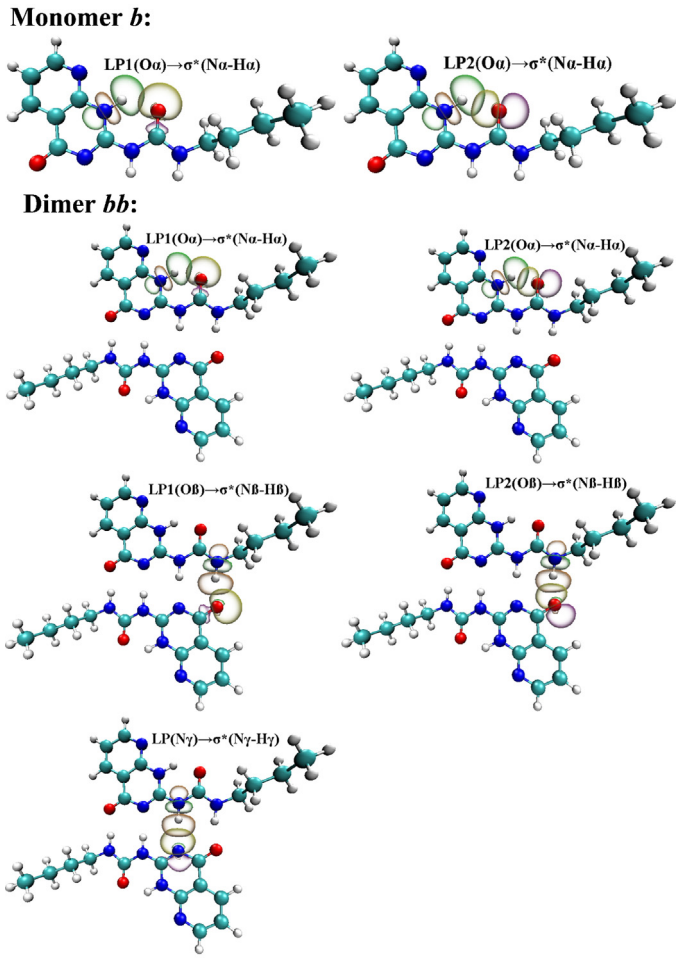

Fig. 5. The interacting donor and acceptor orbitals of the monomer ***b*** and dimer ***bb*** (R = H) at the PBE1PBE/6-311++G (2df,2p) level (vacuum).

general, larger stabilization energy ($E(2)$) corresponds to stronger interaction between donor and acceptor orbital (delocalization) and greater hyperconjugation in multiple and intra hydrogen bonds and even higher stabilization of the system. A case study of **DeAP** monomer in ***b*** form and dimer in ***bb*** form (R = H) in a vacuum was performed to obtain insights into the intramolecular and quadruple hydrogen bonds. It is worth emphasizing that, oxygen atoms have two different values of stabilization energies between its two asymmetric lone pairs (LP) of electron and antibonding orbitals of the donor bond, whereas N atoms only have one value. As shown in Fig. 5 (created using VMD program [54]) and Table 3, stabilization energies for intramolecular hydrogen bonds N—H(α)...O increase after dimerization. In the light of Alabugin's work [55], the hyperconjugation energies of strong H-bonds (>11 kcal/mol) have caused the prolongation of the C—H bonds as well as red shifts. Not surprisingly, the dimer of ***bb*** form studied here also showed such properties, i.e., the prolongation of the N—H bonds (see Table 1 and Table S2). At the meantime, as a result of hyperconjugative interactions in all hydrogen bonds, electron transfers from lone pairs of electron in O or N atoms in acceptor to N—H bonds in donor. Consequently, the occupancies of H-bond donor (antibonding N—H bonds, **σ* (HDB)**) increase, and meanwhile, those of N or O atom with lone pairs (**n**) reduce. Table 3 reveals that the s-character of hybrid orbitals of N atoms (**s(N)**) in donor N—H bonds of intra or intermolecular H-bonds increase after rehybridization because H become more electropositive during this process, which agree with Alabugin's research [55]. Theoretically, rehybridization and

Table 3
NBO Analysis of monomer in ***b*** form and dimer in ***bb*** form (R = H) in a vacuum at PBE1PBE/6-311++G(2df,2p) level[a].

		Q(N)	Q(H)	Q(HAA)	*s* (N)	*n*{LP1 (HAA)}	*n*{LP2 (HAA)}	δn{LP (HAA)}	σ^* (HDB)	$E(2)\{LP_{(HAA)} - \sigma^*_{(N-H)}\}$
b	**N—H (α)...O**	−0.5950	0.4650	−0.6840	29.86%	1.9730	1.8517		0.0381	LP1 (Oα) → σ^* (Nα—Hα):3.16
										LP2 (Oα) → σ^* (Nα—Hα):7.00
	N—H (β)...O	−0.6380	0.3900	−0.6010	26.85%	1.9810	1.8746		0.0170	
	N—H (γ)...N	−0.6420	0.4210	−0.6080	27.23%	1.8943			0.0146	
bb	**N—H (α)...O**	−0.5870	0.4730	−0.7080	29.94%	1.9681	1.8497	−0.0069	0.0551	LP1 (Oα) → σ^* (Nα—Hα):5.63
		[0.0080]	[0.0080]		[0.08%]				[0.0170]	LP2 (Oα) → σ^* (Nα—Hα):13.75
	N—H (β)...O	−0.6450	0.4430	−0.6740	30.60%	1.9647	1.8691	−0.0218	0.0607	LP1 (Oβ) → σ^* (Nβ—Hβ):6.51
		[−0.0070]	[0.0530]		[3.75%]				[0.0437]	LP2 (Oβ) → σ^* (Nβ—Hβ):15.35
	N—H (γ)...N	−0.6600	0.4600	−0.6680	30.44%	1.8762		−0.0181	0.0534	LP1 (Nγ) → σ^* (Nγ—Hγ):15.48
		[−0.0180]	[0.0390]		[3.21%]				[0.0388]	

[a] The variation are listed in square brackets. **HAA** and **HDB** are hydrogen bonding acceptor atom and donor bond, respectively. **Q** is the charge of specified atom.

repolarization may shorten N—H bonds, but they are less competitive to hyperconjugative interactions. The latter possessing enough high interaction energies between hydrogen-bonding acceptors and donor orbitals can result in the prolongation of N—H bonds as well as red shifts of their stretching vibrational modes. That agrees well with the results derived from Table S2 and Table 1.

3.4. AIM topology analysis

The Bader theory, "atoms in molecules" (AIM) [56], was performed here to analyze the topology properties of hydrogen bonds. Among the eight topological criteria proposed by Popelier and Koch [57–59] for the characterization of noncovalent interactions, such as hydrogen bonds, three elements are most widely applied [60], involving: (i) proper topological formats, for instance, the existence of bond critical points (BCPs) with $\lambda_1 \leq \lambda_2 < 0 < \lambda_3$ between hydrogen atoms and hydrogen bonding acceptor atoms; (ii) the electron density $\rho(r)$ of the bond critical point (BCP) for the closed-shell interaction should be in 0.002–0.04 a.u.; (iii) the Laplacian $\nabla^2\rho(r)$ of the electron density of BCPs for the closed-shell interaction should be ranged from 0.02 to 0.15 a.u. Fig. S4 and Table 4 illustrate the molecular graph and topology parameters of bond critical points for the dimer of ***bb*** form (R = H) in a vacuum, respectively. We can see clearly that BCP exists not only in N—H(α)...O, but also in N—H(β)...O and N—H(γ)...N arrays with the following order $\lambda_3 > 0 > \lambda_2 > \lambda_1$. Furthermore, the electron density $\rho(r)$ and Laplacian $\nabla^2\rho(r)$ values of BCPs are within the scope proposed by Popelier and Koch for hydrogen bonding interactions. These results imply that intermolecular hydrogen bonding arrays coexist with the intramolecular ones in the dimer. Once dimers are formed, the dipolar polarization and volume of hydrogen atoms reduce. In the meantime, electrons tend to transfer from the H atoms to the acceptor atoms when forming the H-bonds with the increment of the charge from 0.0216 to 0.1148 a.u. These all strongly suggest the presence of quadruple H-bonds in the dimer. The hydrogen bond energies (E_{HB}) obtained by the Espinosa approach [44] differ much from each other, showing that N—H...O bonds (**α**: −53.95 kJ/mol, **β**: −45.42 kJ/mol) are much stronger than N—H...N bond (−24.94 kJ/mol) in ***bb***. It is interesting to note that, for N—H...O bonds, the intramolecular H-bond is slightly stronger than the intermolecular one, which is in agreement with the data of corresponding H...O bond lengths (Table S2). Therefore, intramolecular H-bonds are also important for the stability of dimers. To get a deeper insight into the nature of interactions in the dimer, we conducted the electronic energy density (H_C) analysis [61] of the BCPs according to

$$H_C = G_C + V_C \tag{3}$$

where G_C is the kinetic energy density, V_C is the potential energy density term, and the relationship between Laplacian values and H_C can be described as [61]

$$\left(\frac{1}{4}\right)\nabla^2\rho(r) = 2G_C + V_C \tag{4}$$

It was proposed that $|V_C|$ is larger than G_C, and H_C is smaller than 0 in bonds with any degree of covalent character, but $H_C > 0$ indicates a merely closed shell interactions [62]. According to Rozas et al. [63], positive H_C and $\nabla^2\rho(r)$ values correspond to weak H-bonds, positive $\nabla^2\rho(r)$ and negative H_C values correspond to moderate ones, whereas negative $\nabla^2\rho(r)$ and H_C values correspond to strong hydrogen-bondings. All Laplacians $\nabla^2\rho(r)$ of electron density at BCPs are positive and the energy density H_C at BCPs are negative for dimers in ***bb*** form in a vacuum studied here (Table 4), indicating the moderate strength and partially covalent nature of hydrogen bonds (the interactions can be seen as not so weak, at least as medium in strength, and as partly covalent in nature) in dimer of ***bb*** form, but the weak hydrogen-bonding nature for monomer in ***b*** form (with positive H_C and $\nabla^2\rho(r)$ values at BCPs).

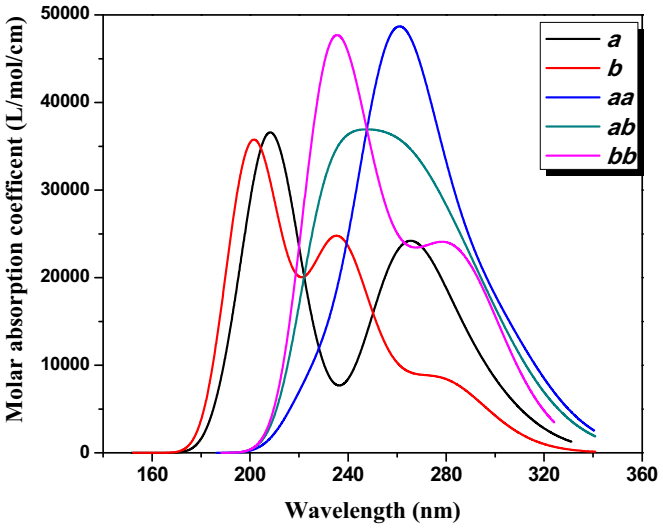

Fig. 6. UV–visible absorption spectra for monomers and dimers at the PBE1PBE/6-311++G(2df,2p) level (in toluene).

3.5. UV–visible and ^{1}H NMR spectroscopy

The Ultraviolet visible spectra analysis of multiple hydrogen-bonding dimers of **DeAP *a*** and its conformers (R = H) has been conducted in chloroform and toluene using the time dependent density functional theory (TD-DFT) at the PBE1PBE/6-311++G(2df,2p) level on the basis of ground-state optimized structures. The wave lengths of three relatively intense electronic transitions (λ), excitation energies, and oscillator (*f*) of singlet excitations are illustrated in Fig. 6 and Table S7. From a theoretical point of view, since the absorption wave lengths are distinctive, UV spectra may be applied for the recognitions of monomers and dimers and the evaluation of dimerization degree. For example, the two intense electronic transitions are determined to be 235.91 nm (f = 0.5707) and 200.85 nm (f = 0.4978) for monomer in ***b*** form, moreover, 281.61 nm (f = 0.2396) and 264.47 nm (f = 0.3332) for dimer in ***ab*** form, but 283.94 nm (f = 0.5249) and 231.84 nm (f = 0.9021) for ***bb*** form in toluene, indicating the red shift of absorption maximum caused by dimerization process. It appears that the results from chloroform are similar to those in toluene, showing that the solvent effect is negligible.

The ^{1}H NMR chemical shifts analysis was also conducted in toluene with GIAO method at the PBE1PBE/6-311++G(2df,2p) level. For comparison with the experiment, the chemical shifts were corrected by TMS. As can be seen from Table S6 and Scheme S3, six N—H signals (R = H) are found for heterodimer in ***ab*** form and three for each homodimer (in ***aa*** and ***bb*** form) at 243 K in toluene, the correlation plot adhere to the linear equation, $Y = 2.45591 + 0.85562X$. The value of correlation coefficient (R^2 = 0.97711) suggests that good agreement has been achieved between computational and experimental chemical shifts although there is some deviation from ideal situation here. Therefore, the PBE1PBE functional can give relatively accurate results for dealing with molecules based on multiple hydrogen bonds. For instance, the calculated chemical shifts of dimers in ***bb*** form are 14.523, 11.512, 12.281 ppm, respectively, which are similar to the experimental ones (13.950, 10.570, and 11.890 ppm). According to Table S6, downfield shifts during the dimerization process obtained from calculations may provide important information for related investigations in future.

Table 4
Topology analysis of **BCPs** (E_{HB}: kJ/mol) and H atoms for hydrogen bonds in monomer ***b*** and dimer ***bb*** at the PBE1PBE/6-311++G(2df,2p) level[a] (vacuum) (R = H).

		BCP									H atom		
		$\rho(r)$	$\nabla^2\rho(r)$	λ_1	λ_2	λ_3	G_r	V_r	E_{HB}	H_c	V	Q_H	M
b	**N—H (α)...O**	0.0324	0.1164	−0.0445	−0.0425	0.2033	0.0279	−0.0266	−34.92	0.0012	19.3791	0.5336	0.1530
	N—H (β)...O										29.9994	0.4049	0.1853
	N—H (γ)...N										27.7881	0.4494	0.1752
bb	**N—H (α)...O**	0.0452	0.1424	−0.0707	−0.0689	0.2820	0.0384	−0.0411	−53.95	−0.0028	16.9519	0.5552	0.1314
											[−2.4272]	[0.0216]	[−0.0216]
	N—H (β)...O	0.0407	0.1158	−0.0660	−0.0643	0.2461	0.0318	−0.0346	−45.42	−0.0028	16.0617	0.5197	0.1269
											[−13.9377]	[0.1148]	[−0.0584]
	N—H (γ)...N	0.0285	0.0703	−0.0397	−0.0379	0.1480	0.0183	−0.0190	−24.94	−0.0007	18.0809	0.5073	0.1609
											[−9.7072]	[0.0580]	[−0.0143]

[a] The variation are listed in square brackets. **V**, $\mathbf{Q_H}$, and **M** are the volume, charge, and dipolar polarization of the hydrogen atom.

4. Conclusions

In this paper, we have performed a theoretical DFT study on a series of dimers based on **DeAP *a*** and its conformers with different substituents adjacent to the quadruple hydrogen bonds. Our computations clearly show that monomers in ***a*** form have the lowest energy in various environments (vacuum, toluene, chloroform, and water), and mostly, from the view of binding energy and free energy, dimers in ***bb*** form are more favorable than other forms. It is found that the sequence of stability for dimer is ***bb*** > ***ab*** > ***aa*** > ***cc***. Substituents can bring about lower energy for ***ab*** form, accordingly increase its ratio in the equilibrium system. That is in accordance with the experiment results. Intermolecular and intramolecular H-bonds can be confirmed by geometrical and topological analyses. Explorations of frequency and NBO indicate that these hydrogen bonds exhibit substantially decreased stretching frequencies and red shift of IR spectrum. Moreover, we found that larger substituents may result in more favorable free energies and further promote the dimerization process in ***bb*** form, though they may lead to slightly smaller binding energies in different conditions. Solvent effects calculations using the implicit solvent model and the implicit–explicit solvent model suggest that dimerization can be promoted in weakly polar solvent such as toluene and chloroform, whereas prevented in polar water for the competitive interactions between monomers and water molecules. The UV–visible spectra exhibit the obvious difference of maximum absorption wavelengths between monomers and dimers, and therefore can be used as a powerful tool to identify intermolecular hydrogen bonds of **DeAP *a*** equilibrium systems. ^{1}H NMR chemical shifts analysis further verified the available experimental data for dimers. Downfield shifts during dimerization obtained from computations provide important information for related researches in future. Good agreements with various experimental results prove that economic PBE1PBE functional combining with 6-31G(d) and 6-311++G(2df,2p) basis sets performed well on describing the nature and property of multiple hydrogen bonds of such supramolecular dimers. These results provide a perspective toward the construction of stable hydrogen-bonded networks in weak polar solvents based on **DeAP *a***. More efforts may be made on increasing H-bonds sites or building new functional networks to improve the stability of hydrogen-bonded dimers in polar solvents.

Acknowledgements

We thank the reviewers for their comments. This research was supported by National Natural Science Foundation of China (No. 51203016 and 21303011), National High Technology Research and Development Program of China (No. SS2012AA110301 and 2013AA110103) and Program for New Century Excellent Talents in University (No. NCET-12-0816).

Appendix A. Supplementary data

Supplementary data associated with this article can be found, in the online version, at http://dx.doi.org/10.1016/j.jmgm.2015.03.004.

References

[1] (a) L. Brunsveld, B. Folmer, Chem. Rev. 101 (2001) 4071;
(b) D.A. Leigh, C.C. Robertson, A.M.Z. Slawin, P.I.T. Thomson, J. Am. Chem. Soc. 135 (2013) 9939–9943.
[2] (a) P.S. Corbin, S.C. Zimmerman, P.A. Thiessen, N.A. Hawryluk, T.J. Murray, J. Am. Chem. Soc. 123 (2001) 10475–10488;
(b) B.A. Blight, C.A. Hunter, D.A. Leigh, H. McNab, P.I.T. Thomson, Nat. Chem. 3 (2011) 244–248.
[3] L.J. Prins, D.N. Reinhoudt, P. Timmerman, Angew. Chem. Int. Ed. 40 (2001) 2382–2426.
[4] Y. Chen, A.M. Kushner, G.A. Williams, Z. Guan, Nat. Chem. 4 (2012) 467–472.
[5] D.C. Sherrington, K.A. Taskinen, Chem. Soc. Rev. 30 (2001) 83–93.
[6] C.A. Anderson, A.R. Jones, E.M. Briggs, E.J. Novitsky, D.W. Kuykendall, N.R. Sottos, S.C. Zimmerman, J. Am. Chem. Soc. 135 (2013) 7288–7295.
[7] W. Binder, R. Zirbs, in: W. Binder (Ed.), Hydrogen Bonded Polymers, vol. 207, Springer, Berlin, Heidelberg, 2007, pp. 1–78.
[8] T. Aida, E.W. Meijer, S.I. Stupp, Science 335 (2012) 813–817.
[9] A.J. Wilson, Soft Matter 3 (2007) 409–425.
[10] P.Y. Dankers, E. Meijer, Bull. Chem. Soc. Jpn. 80 (2007) 2047–2073.
[11] T.F.A. de Greef, E.W. Meijer, Nature 453 (2008) 171–173.
[12] (a) T.F. De Greef, M.M. Smulders, M. Wolffs, A.P. Schenning, R.P. Sijbesma, E. Meijer, Chem. Rev. 109 (2009) 5687–5754;
(b) M. Krische, J.-M. Lehn, in: M. Fuiita (Ed.), Molecular Self-Assembly Organic Versus Inorganic Approaches, vol. 96, Springer, Berlin, Heidelberg, 2000, pp. 3–29;
(c) A. Gooch, N.S. Murphy, N.H. Thomson, A.J. Wilson, Macromolecules 46 (2013) 9634–9641;
(d) Y. Li, T. Park, J.K. Quansah, S.C. Zimmerman, J. Am. Chem. Soc. 133 (2011) 17118–17121.
[13] (a) S.K. Yang, S.C. Zimmerman, Isr. J. Chem. 53 (2013) 511–520;
(b) A. Gooch, C. Nedolisa, K.A. Houton, C.I. Lindsay, A. Saiani, A.J. Wilson, Macromolecules 45 (2012) 4723–4729.
[14] C. Fouquey, J.-M. Lehn, A.-M. Levelut, Adv. Mater 2 (1990) 254–257.
[15] T. Kato, P.G. Wilson, A. Fujishima, J.M.J. Frechet, Chem. Lett. 19 (1990) 2003–2006.
[16] A.J. Wilson, Nat. Chem. 3 (2011) 193–194.
[17] (a) R.P. Sijbesma, F.H. Beijer, L. Brunsveld, B.J.B. Folmer, J.H.K.K. Hirschberg, R.F.M. Lange, J.K.L. Lowe, E.W. Meijer, Science 278 (1997) 1601–1604;
(b) F.H. Beijer, R.P. Sijbesma, H. Kooijman, A.L. Spek, E.W. Meijer, J. Am. Chem. Soc. 120 (1998) 6761–6769.
[18] R.F.M. Lange, M. Van Gurp, E.W. Meijer, J. Polym. Sci., Part A: Polym. Chem. 37 (1999) 3657–3670.
[19] V.G.H. Lafitte, A.E. Aliev, P.N. Horton, M.B. Hursthouse, K. Bala, P. Golding, H.C. Hailes, J. Am. Chem. Soc. 128 (2006) 6544–6545.
[20] (a) P.S. Corbin, S.C. Zimmerman, J. Am. Chem. Soc. 120 (1998) 9710–9711;
(b) P.S. Corbin, L.J. Lawless, Z. Li, Y. Ma, M.J. Witmer, S.C. Zimmerman, Proc. Natl. Acad. Sci. U. S. A. 99 (2002) 5099–5104.
[21] E.M. Todd, S.C. Zimmerman, J. Am. Chem. Soc. 129 (2007) 14534–14535.
[22] P.S. Corbin, S.C. Zimmerman, J. Am. Chem. Soc. 122 (2000) 3779–3780.
[23] T. Park, S.C. Zimmerman, S. Nakashima, J. Am. Chem. Soc. 127 (2005) 6520–6521.
[24] M.F. Mayer, S. Nakashima, S.C. Zimmerman, Org. Lett. 7 (2005) 3005–3008.
[25] M. Pfleiderer, W. Pfleiderer, Heterocycles 33 (1992) 905–929.
[26] (a) S. Schlund, C. Schmuck, B. Engels, J. Am. Chem. Soc. 127 (2005) 11115–11124;
(b) I. Alkorta, J. Elguero, S. Goswami, R. Mukherjee, J. Chem. Soc., Perkin Trans. 2 (2002) 894–898;

(c) H. Sun, H.H. Lee, I. Blakey, B. Dargaville, T.V. Chirila, A.K. Whittaker, S.C. Smith, J. Phys. Chem. B 115 (2011) 11053–11062;
(d) H. Dong, W. Hua, S. Li, J. Phys. Chem. A 111 (2007) 2941–2945;
(e) W. Xu, X.-C. Li, H. Tan, G.-J. Chen, Phys. Chem. Chem. Phys. 8 (2006) 4427–4433.
[27] M.-D. Su, S.-Y. Chu, J. Am. Chem. Soc. 121 (1999) 4229–4237.
[28] (a) N. Iche-Tarrat, J.-C. Barthelat, A. Vigroux, J. Phys. Chem. B 112 (2008) 3217–3221;
(b) P.C. Gomez, O. Galvez, R. Escribano, Phys. Chem. Chem. Phys. 11 (2009) 9710–9719.
[29] J.P. Perdew, K. Burke, M. Ernzerhof, Phys. Rev. Lett. 78 (1997) 1396.
[30] S.M. Bachrach, J. Phys. Chem. A 112 (2008) 3722–3730.
[31] A.D. Rabuck, G.E. Scuseria, Theor. Chem. Acc 104 (2000) 439–444.
[32] M. Ernzerhof, G.E. Scuseria, J. Chem. Phys. 110 (1999) 5029–5036.
[33] Y. Zhao, D.G. Truhlar, J. Chem. Theory Comput. 1 (2005) 415–432.
[34] X. Xu, W.A. Goddard, P. Natl, Acad. Sci. U. S. A. 101 (2004) 2673–2677.
[35] Y. Zhao, D. Truhlar, Theor. Chem. Acc. 120 (2008) 215–241.
[36] J.-D. Chai, M. Head-Gordon, Phys. Chem. Chem. Phys. 10 (2008) 6615–6620.
[37] (a) A.D. Becke, Phys. Rev. A 38 (1988) 3098–3100;
(b) C. Lee, W. Yang, R.G. Parr, Phys. Rev. B 37 (1988) 785–789.
[38] M. Frisch, G. Trucks, H.B. Schlegel, G. Scuseria, M. Robb, J. Cheeseman, G. Scalmani, V. Barone, B. Mennucci, G. Petersson, Gaussian 09, Revision A.02, Gaussian, Inc., Wallingford, CT, 2009.
[39] S. Miertuš, E. Scrocco, J. Tomasi, Chem. Phys. 55 (1981) 117–129.
[40] S. Miertus˜, J. Tomasi, Chem. Phys. 65 (1982) 239–245.
[41] S.F. Boys, F. Bernardi, Mol. Phys. 19 (1970) 553–566.
[42] S. Simon, M. Duran, J.J. Dannenberg, J. Chem. Phys. 105 (1996) 11024–11031.
[43] T. Lu, F. Chen, J. Comput. Chem. 33 (2012) 580–592.
[44] E. Espinosa, E. Molins, C. Lecomte, Chem. Phys. Lett. 285 (1998) 170–173.
[45] A. Becke, C.F. Matta, R.J. Boyd, The Quantum Theory of Atoms in Molecules: From Solid State to DNA and Drug Design, John Wiley & Sons, 2007.
[46] G.A. Jeffrey, An Introduction to Hydrogen Bonding, vol. 12, Oxford University Press, New York, 1997.
[47] L. Pauling, The Natune of the Chemical Bond and the Structure of Molecules and Crystals: An Introduction to Modern Structural Chemistry, vol. 18, Cornell University Press, 1960.
[48] F.H. Beijer, R.P. Sijbesma, H. Kooijman, A.L. Spek, E.W. Meijer, J. Am. Chem. Soc. 120 (1998) 6761–6769.
[49] (a) B. Ośmiałowski, E. Kolehmainen, M. Kowalska, J. Org. Chem. 77 (2012) 1653–1662;
(b) B. Ośmiałowski, E. Kolehmainen, S. Ikonen, A. Valkonen, A. Kwiatkowski, I. Grela, E. Haapaniemi, J. Org. Chem. 77 (2012) 9609–9619;
(c) B. Osímiałowski, E. Kolehmainen, R. Gawinecki, R. Dobosz, R. Kauppinen, J. Phys. Chem. A 114 (2010) 12881–12887;
(d) B. Ośmiałowski, E. Kolehmainen, R. Kauppinen, M. Kowalska, Supramol. Chem. 23 (2011) 579–586;
(e) B. Ośmiałowski, E. Kolehmainen, E. Kalenius, B. Behera, R. Kauppinen, E. Sievänen, Struct. Chem. 22 (2011) 1143–1151.
[50] A.N. Alexandrova, W.L. Jorgensen, J. Phys. Chem. B 111 (2007) 720–730.
[51] J. Přecechtělová, M.L. Munzarová, P. Novák, V. Sklenář, J. Phys. Chem. B 111 (2007) 2658–2667.
[52] A.V. Marenich, C.J. Cramer, D.G. Truhlar, J. Chem. Theory Comput. 6 (2010) 2829–2844.
[53] J. Chocholousova, V. Spirko, P. Hobza, Phys. Chem. Chem. Phys. 6 (2004) 37–41.
[54] W. Humphrey, A. Dalke, K. Schulten, J. Mol. Graph. Model. 14 (1996) 33–38.
[55] I.V. Alabugin, M. Manoharan, S. Peabody, F. Weinhold, J. Am. Chem. Soc. 125 (2003) 5973–5987.
[56] R.F.W. Bader, Chem. Rev. 91 (1991) 893–928.
[57] U. Koch, P.L.A. Popelier, J. Phys. Chem. 99 (1995) 9747–9754.
[58] P.L.A. Popelier, J. Phys. Chem. A 102 (1998) 1873–1878.
[59] P. Popelier, F. Aicken, S. O'Brien, Chem. Model. Appl. Theory 1 (2000) 143–198.
[60] P. Lipkowski, S.J. Grabowski, T.L. Robinson, J. Leszczynski, J. Phys. Chem. A 108 (2004) 10865–10872.
[61] R.F. Bader, Acc. Chem. Res. 18 (1985) 9–15.
[62] (a) W.D. Arnold, E. Oldfield, J. Am. Chem. Soc. 122 (2000) 12835–12841;
(b) S. Jenkins, I. Morrison, Chem. Phys. Lett. 317 (2000) 97–102.
[63] I. Rozas, I. Alkorta, J. Elguero, J. Am. Chem. Soc. 122 (2000) 11154–11161.